Simulation of Guided Wave Interaction with In-Plane Fiber Waviness

Cara A.C. Leckey[1, a)] and Peter D. Juarez[1,b)]

[1]NASA Langley Research Center, Hampton, VA, 23681 USA

[a)]Corresponding author: cara.ac.leckey@nasa.gov
[b)]peter.d.juarez@nasa.gov

Abstract. Reducing the timeline for certification of composite materials and enabling the expanded use of advanced composite materials for aerospace applications are two primary goals of NASA's Advanced Composites Project (ACP). A key a technical challenge area for accomplishing these goals is the development of rapid composite inspection methods with improved defect characterization capabilities. Ongoing work at NASA Langley is focused on expanding ultrasonic simulation capabilities for composite materials. Simulation tools can be used to guide the development of optimal inspection methods. Custom code based on elastodynamic finite integration technique is currently being developed and implemented to study ultrasonic wave interaction with manufacturing defects, such as in-plane fiber waviness (marcelling). This paper describes details of validation comparisons performed to enable simulation of guided wave propagation in composites containing fiber waviness. Simulation results for guided wave interaction with in-plane fiber waviness are also discussed. The results show that the wavefield is affected by the presence of waviness on both the surface containing fiber waviness, as well as the opposite surface to the location of waviness.

INTRODUCTION

Composite materials are commonly used by the aerospace industry in order to enable lightweight advanced aircraft and spacecraft designs. However, the current timeline for development and certification of composite structures is around a decade [1]. NASA's Advanced Composites Project has the goal of reducing the timeline for certification of composite materials and structures [2]. Nondestructive inspection is a key requirement that can impact composite certification timelines. Rapid nondestructive evaluation (NDE) techniques are needed to quantify and characterize defects/damage in aerospace composites. Carbon fiber reinforced polymer (CFRP) composite defects can be created during the manufacturing process in layup and/or curing stages. Additionally, damage to composites can occur in the post-cure stage when components are relocated, altered, and/or attached to other components. Manufacturing defects occurring in the layup or curing stages include fiber waviness (in-plane/marcelling and out-of-plane/wrinkling), fiber misalignment, porosity, foreign object damage (FOD), and disbonds. Damage occurring in a manufacturing setting post-cure include defects such as delaminations due to tool drops and other unintended loads placed on the component. These types of defects can reduce the strength/stiffness of the material, affecting the reliability and durability of composite parts [3, 4]. For the two categories of fiber waviness defects (in-plane and out-of-plane), both can be induced by temperature gradients during curing [5]. Wrinkling can also be created during layup of complex geometry parts. Additionally, it has been reported that wrinkling can be converted to in-plane waviness during the curing process [6]. Wrinkling defects are more readily visible to the human eye since they create an out-of-plane change in the material surface/thickness.

Ultrasonic inspection is one of the most common NDE techniques for quantification of damage in composites. The use of ultrasonic guided waves (GW) for large area inspection of composites has been widely studied in recent years for both metallic and composite materials. A common approach for GW inspection is to attach/bond multiple

contact piezoelectric sensors to a component in order to send and receive ultrasonic waves. The multi-sensor approach is often used in tomography, phased array, and sparse array setups, along with the associated data processing approaches [7-9]. Another popular approach involves use of a single excitation source, such as a single contact transducer, air-coupled transducer or through use of laser ultrasonic methods. The single source approach is often combined with noncontact wavefield measurements using laser Doppler vibrometry (LDV) or air-coupled transducers [10]. The noncontact measurement approach involves point-by-point scanning combined with data processing methods such as instantaneous or local wavenumber techniques [11, 12]. In recent years progress has also been made towards more rapid noncontact GW inspections via a variety of methods for reducing scan times [13-16]. Much of the prior GW work in composite materials focuses on detection of delamination and disbond type defects.

Recent work at NASA Langley has focused on the application of GW techniques for detection and characterization of manufacturing defects in composites. The work presented in this paper is focused on GW interaction with in-plane fiber waviness. Preliminary investigations reported in prior literature have found that GWs are affected by fiber waviness, and undergo a very small change in velocity when encountering such defects [17]. In-plane waviness presents a detectability/characterization challenge for several reasons: 1) it is not readily visible to the eye, 2) the defect can occur interior to the composite while causing no surface indication, 3) compared to defects such as delaminations, in-plane waviness has a much smaller effect on typical NDE methods such as ultrasound. Another key challenge for developing waviness detection and quantification methods is that it is difficult to create representative NDE standards for experimental testing. Simulation tools are therefore particularly useful in guiding the development of detection and quantification techniques. In this work elastodynamic finite integration technique (EFIT) has been implemented to simulate wave interaction with in-plane fiber waviness. The following sections describe the simulation approach, methodology used to incorporate waviness, model validation efforts, and an example case showing GW interaction with the waviness type defect.

WAVINESS MODELING

Elastodynamic Finite Integration Technique

Various mathematical approaches exist for modeling ultrasonic wave propagation in elastic materials. Analytical methods are generally limited in the types of cases they can accurately represent and frequently rely on simplifying approaches such as Born or Kirchoff approximations [18]. Numerical methods are often used in cases involving complex damage geometries, complex specimen geometry/structure and/or non-isotropic material properties. Common numerical methods include finite element analysis (FEA), finite difference (FD), and finite integration technique (FIT). EFIT is a numerical method similar to staggered-grid finite difference techniques. The technique has been in use since the 1990s with extensive foundational work reported by authors such as Fellinger, Marklein, and Schubert, among others [19-22]. In this paper EFIT is implemented to study wave interaction with in-plane fiber waviness defects. The EFIT equations implemented for this work are in Cartesian coordinates and the simulation uses a cubic grid discretization for calculating the stresses and velocities at all spatial points in the 3-dimensional (3D) simulation. The code is explicitly parallelized to run efficiently on cluster or multicore computing resources using Message Passing Interface (MPI).

Prior code validation studies for orthotropic ply layups and additional discussion about EFIT for composites can be found in previous work by the authors [23]. Since prior validation work focused on orthotropic cases, additional verification and validation studies were required in order to establish confidence in the anisotropic EFIT custom code for representing fiber waviness. In the section below, the general approach for incorporating in-plane waviness is described. Following this description, validation comparisons that check the physics involved in the waviness case are presented.

Mathematical Approach to Model Waviness

The anisotropic EFIT code accounts for the anisotropic material properties of each individual ply layer by including the appropriate stiffness matrices for each ply rotation. In addition, the custom simulation code allows direct control over the stiffness matrix at every grid point in the 3D simulation space. The incorporation of in-plane waviness (marcelling) is therefore implemented using the appropriately rotated stiffness matrix at each grid point location corresponding to fiber waviness (see Fig. 1). As a general description, waviness is represented by a function, $f(x, y, z)$, which depends on spatial location in x, y, z. For the cases studied in this paper, it was assumed that the wavy fibers

follow the same functional form in the y direction, i.e., waviness becomes a function of only *x* and *z*, *f(x,z)*. For each *z* location (depth) the tangent to the curve is found at all points along the curve and the corresponding rotation angle is defined as:

$$\theta_{x,z} = tan^{-1}\left(\frac{f(x_2,z)-f(x_1,z)}{(x_2-x_1)}\right) \quad (1)$$

where the 0 degree fiber direction is taken as $\theta_{x,z} = 0$. The stiffness matrix is rotated by the appropriate $\theta_{x,z}$ at each grid point in the simulation.

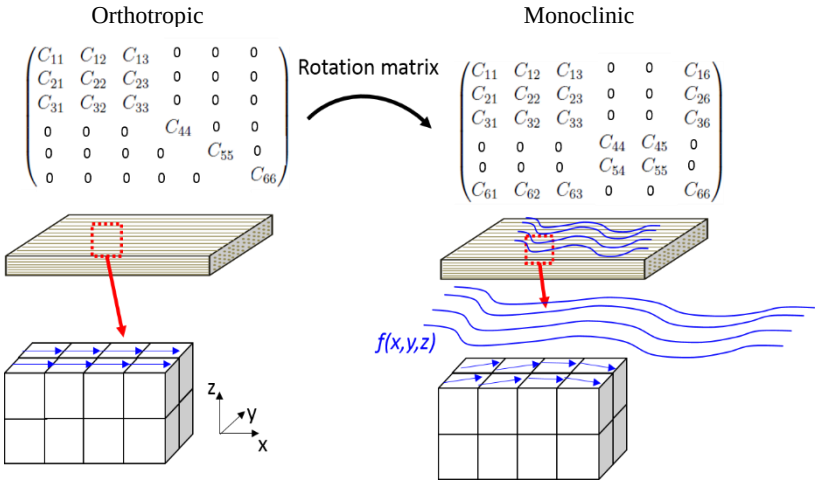

FIGURE 1. Diagram of process for calculating the angle of in-plane fiber waviness to be included in the custom ultrasound simulation. Waviness is defined by a function *f(x, z)*. At each simulation grid location the stiffness matrix is rotated according to equation (1).

Validation Comparisons

As shown in Fig. 1, mathematically incorporating in-plane fiber waviness requires stiffness matrix rotations that are not orthotropic. Monoclinic stiffness matrices must be incorporated into the simulation and the additional non-zero terms in the stiffness matrix mean that the EFIT equations include terms that were zero for orthotropic cases. This additional mathematics requires the appropriate verification and validation comparisons to establish confidence that the additional EFIT terms are implemented as intended and represent the correct physics. In prior work, a wavenumber based method was used for a quantitative validation comparison between EFIT and experiment [23]. This approach entails the use of LDV to record experimental wavefield data. As described in that prior publication, a 3D Fourier Transform is applied to the wavefield data set to transform the 3D data from space-time domain (which has two spatial dimensions, *x* and *y*) to frequency-wavenumber domain. The frequency slice corresponding to the excitation frequency can then be plotted to show the x-direction wavenumber versus the y-direction wavenumber (*kx* vs. *ky*). This approach allows for a quantitative comparison of GW modes between experiment and simulation for all propagation directions.

In this work, experimental data for validation comparisons was collected using a 1D Polytec OFV-505 LDV connected to an OFV-5000 controller system. The LDV was mounted on a motorized scanner for automated 2D grid scans and the LDV was set up normal to the specimen surface, allowing for collection of out-of-plane velocity data. To check the monoclinic EFIT terms, we studied the wavenumber results for an EFIT case of a 30 degree fiber angle CFRP plate, as shown in Fig. 2. Since a 30 degree fiber angle plate was unavailable in the experimental study, the 30 degree EFIT out-of-plane result was compared to the experimental wavenumber data for a unidirectional plate. Such a comparison is sensible for this simple case that includes only a single fiber direction since we expect the 30 degree *kx* vs *ky* result to be a 30 degree rotation of the experimental unidirectional case. Experimental data was collected on an 8-ply, ~0.95 mm thick unidirectional CFRP plate made of IM7/8552 material [23]. A 200 kHz 6.5 cycle Hann windowed sine wave was excited over a circular 0.5 inch diameter contact transducer. The EFIT simulations also

used a 200 kHz 6.5 cycle Hann windowed excitation. The EFIT step size for all simulation cases in this paper was set to 118.6 microns ($\lambda_{min}/33$).

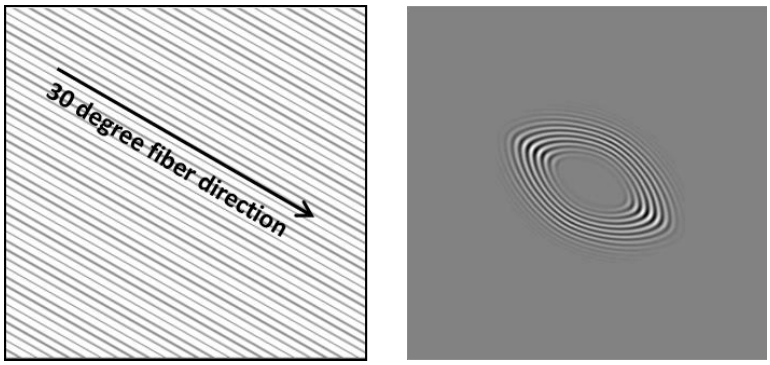

FIGURE 2. Left: Diagram showing 30 degree fiber angle CFRP plate case that corresponds to the monoclinic EFIT simulation case; Right: Single snapshot in time of the A_0 propagation in the 30 degree fiber angle EFIT simulation. Note that the S_0 mode is also present but cannot be seen with the colormap scaling used in the figure.

Figure 3a shows the experimental wavenumber plot at the 200 kHz excitation frequency. Figure 3b shows the EFIT simulation 200 kHz out-of-plane wavenumber result for the exact same case as the experimental data, a unidirectional (0 degree fiber angle) 8-ply CFRP. Figure 3c shows the 200 kHz EFIT simulation out-of-plane wavenumber result for the 30 degree fiber angle case. For this out-of-plane motion case, only the A_0 mode is visible in the wavenumber plots. As expected, the 30 degree wavenumber result is simply a 30 degree rotation of the 0 degree fiber angle case. As shown in the figure, the simulation results agree well with the experimental data. The experiment predicts a slightly lower wavenumber in the *y*-direction, as discussed further in [23]. We also note that the thickness of the *kx*-*ky* 'ring' decreases as the simulation is run longer in time (or experimental data is collected longer in time). Due to the availability of computational resources, the 30 degree simulation was run to a slightly shorter length in time compared to the case in Fig. 3b and therefore has a larger ring thickness.

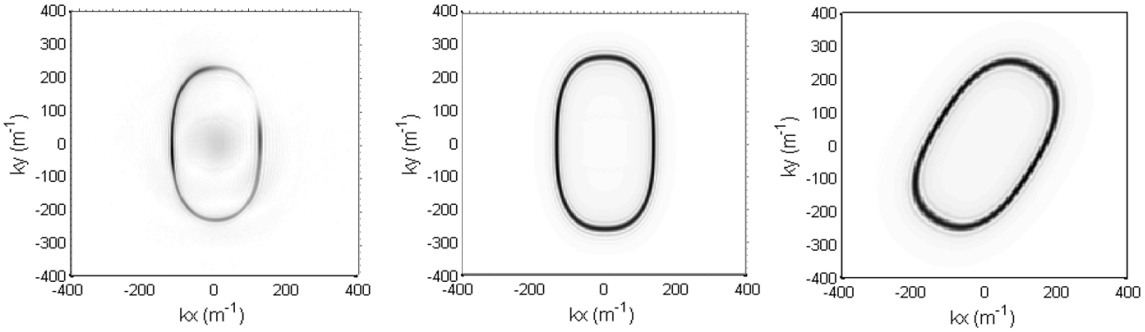

(a) (b) (c)

FIGURE 3. Out-of-plane wavenumber *kx* vs *ky* plots for validation comparison to experiment: (a) Experimental result for a unidirectional plate (note: 0 degree fiber direction is along *ky*=0), (b) EFIT result for a unidirectional plate, (c) EFIT result for 30 degree fiber angle plate (note: 30 degree fiber direction is along thinnest cross-section of ring).

While the 1D LDV setup does not allow for in-plane comparisons to simulation, comparisons between EFIT and dispersion curve predictions were performed. Figure 4 shows EFIT wavenumber plots of in-plane motion for both a unidirectional and 30 degree fiber angle case. S_0, A_0 and SH_0 modes are labeled in the wavenumber plots. The 30 degree case again shows the expected rotation compared to the unidirectional case. For validation purposes, dispersion curves were created for the 30 degree fiber angle case using the spectral method described in [24]. Comparisons between EFIT results and the dispersion curves are given in Table 1.

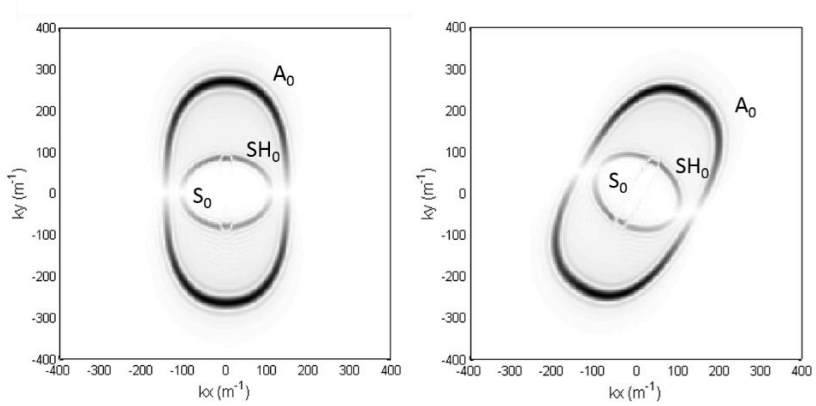

FIGURE 4. In-plane wavenumber results from the EFIT simulation. Left: Unidirectional case with fibers in the 0 degree direction (fiber direction corresponds to *ky*=0). Right: 30 degree fiber angle case.

TABLE 1. In-plane motion wavenumber comparisons between dispersion curve predictions and EFIT for the 30 degree rotation case. Results shown below are for the propagation direction along the fibers. Dispersion curves provided by Imperial College London.

Mode	EFIT k (m^{-1})	Dispersion Curves k (m^{-1})	Percent Difference %
S_0	20.8	19.1	8.52
A_0	145.5	142.6	2.01
SH_0	107.6	108.9	1.20

Fiber Waviness Simulation

Various authors have studied fiber waviness in CFRP composites and the scientific literature was used to define a degree of fiber waviness that is relevant for CFRP composites. The amount of fiber waviness in a CFRP composite can be defined by the amplitude of the fiber wave and the associated wavelength. Mizukami recently reported eddy current based detection of CFRP fiber waviness. For those studies representative waviness samples were created where the level of waviness was measured at an amplitude of A = 1.1 mm over a wavelength of λ=15.9 mm [6]. Fuhr and colleagues have reported degrees of waviness ranging from A=0.6 mm and λ=20 mm to A=1.5 mm and λ=10 mm [25]. Fuhr found that increased amplitude leads to decreases in stiffness and strength.

For the simulation studies in this section, in-plane fiber waviness was defined with A=2 mm and λ=16 mm in the functional form of a 2-cycle cosine wave. An 8-ply thick unidirectional laminate was simulated and fiber waviness was included in a small area in the top ply. The region containing fiber waviness is shown in Fig. 5. Figure 6

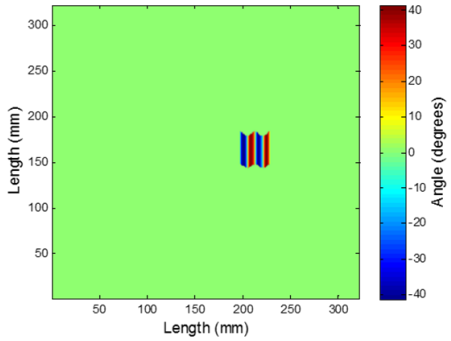

FIGURE 5. Diagram showing the location of fiber waviness in the simulated CFRP laminate. The colorscale represents the stiffness matrix rotation angle versus position.

shows two different snapshots in time of the out-of-plane velocity from the EFIT simulation. The figure shows guided wave modes interacting with the fiber waviness region. Wave interaction with the wavy region can be observed in the figure (inside the regions circled in red). At the earlier point in time, t=29.5 μs after the excitation, the S_0 mode has interacted with the wavy region and waviness effects are observed in the area of the laminate that contains waviness

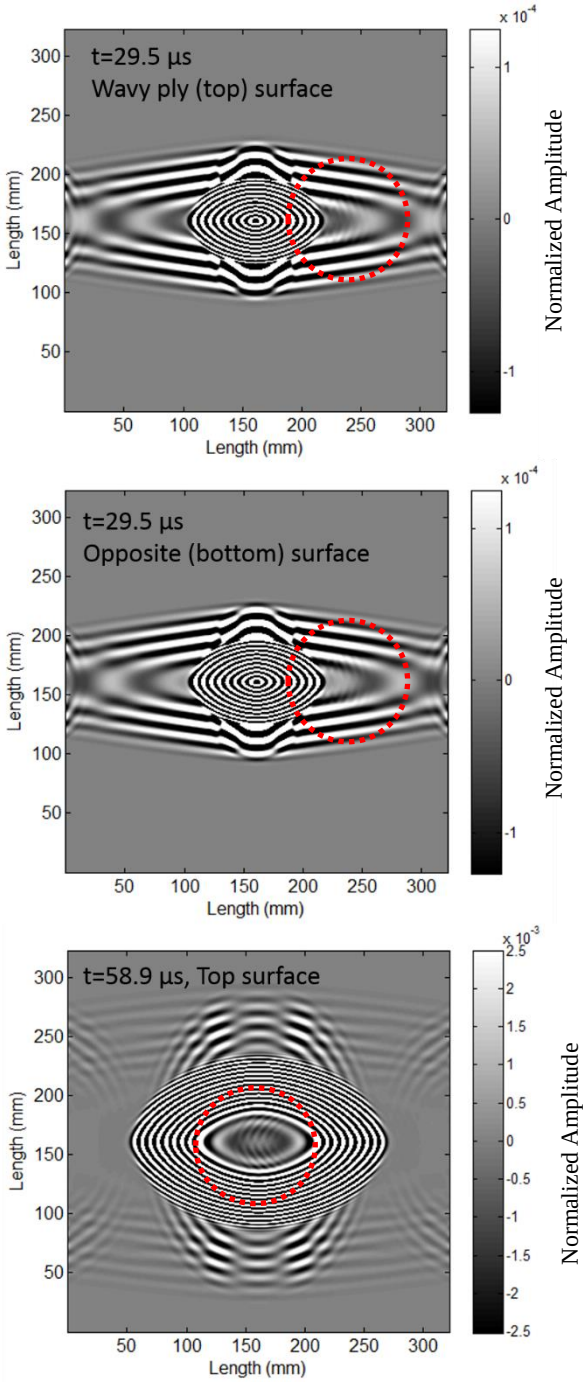

FIGURE 6. EFIT out-of-plane velocity results for two different points in time after the excitation (times as labeled and image correspond to plate surfaces as labeled). The red dashed circles highlight regions of the wavefield where the effects of fiber waviness are visible as 'ripples' in the wavefield.

(visible as 'ripples' in the wavefield). The second image at t=29.5 μs shows the wavefield at the laminate surface opposite to the wavy ply. The image demonstrates that while the waviness region is in the 'top' ply only, the effect of waviness is also visually observed at the back surface of the composite laminate. By t=58.9 μs the A_0 mode has started to interact with the wavy region and reflections from the S_0 mode interaction are visible as reflections moving leftward in the center of the image (circled in red). Based on the wavelength observed in these reflections, it also appears that S_0 to A_0 mode conversion may occur when the S_0 waves interact with the fiber waviness region. Additionally, though not pictured above, it is noted that the reflections at t=58.9 μs were also visible at the laminate surface opposite to the wavy ply.

Various data analysis methods can be applied to wavefield data, such as the type of data simulation data shown above. Methods such as wavenumber analysis and wavenumber domain filtering are commonly applied to such data sets in order to create damage/defects maps. Additional analysis of the above waviness case can be found in [26]. That work also describes results for a cross-ply fiber waviness simulation case.

CONCLUSION

This paper describes recent code validation work to expand EFIT based simulation tools to model ultrasound interaction with in-plane fiber waviness defects. The importance of such validation steps was discussed and results from wavenumber domain comparisons between experiment, dispersion curves, and EFIT have been presented. A mathematical approach for simulating guided wave interaction with in-plane fiber waviness has also been presented, along with results from an example case of in-plane fiber waviness in a unidirectional CFRP laminate. The results in this paper show that waviness has an effect on the guided waves throughout the composite thickness and that S_0 to A_0 mode conversion may occur at the location of fiber waviness. Further studies are required to assess mode conversion and any related data processing methods that may leverage this behavior.

Future work will focus on simulation-guided data analysis methods to create damage maps of manufacturing defects such as fiber waviness. Preliminary work in this area is described in [25], and has shown that unlike delamination damage, new wavenumbers are not expected in waviness regions. Future work will instead focus on methods for detecting the changes in energy directionality and/or mode conversion behavior that has been observed in the simulation studies. Further work will also include experimental studies using laser Doppler vibrometry to assess wavefield changes due to waviness defects in experimental specimens.

ACKNOWLEDGMENTS

The authors would like to specially thank Professor Michael Lowe and Francisco Hernando Quintanilla from Imperial College London for providing dispersion curve data for the in-plane wavenumber comparisons presented in this paper.

REFERENCES

1. G. Warwick, "NASA Led Consortium Will Bring Science to Art of Composites," Aviation Week and Space Technology, http://aviationweek.com/technology/nasa-led-consortium-will-bring-science-art-composites (2015)
2. NASA ARMD, "Advanced Air Vehicles Program, Advanced Composites Project," http://www.aeronautics.nasa.gov/aavp/ac/index.html (2016)
3. I. Daniel, O. Ishai, "Engineering mechanics of composite materials", 2nd Ed, New York: Oxford University Press. (2006)
4. P. Joyce, and T. Moon, "Compression strength reduction in composites with in-plane fiber waviness," Composite Materials: Fatigue and Fracture: 7th Volume. ASTM International. (1998)
5. Z. Su, L. Ye, and Y. Lu, "Guided Lamb waves for identification of damage in composite structures: A review," Journal of sound and vibration 295(3): 753-780. (2006)
6. K. Mizukami, Y. Mizutani, A. Todoroki, Y. Suzuki, "Detection of in-plane and out-of-plane fiber waviness in unidirectional carbon fiber reinforced composites using eddy current testing," Composites Part B: Engineering. 86:84-94. (2016)

7. K. Çınar, N. Ersoy, “Effect of fibre wrinkling to the spring-in behaviour of L-shaped composite materials,” Composites Part A: Applied Science and Manufacturing. 69:105-14 (2015)
8. S.M. Prasad, K. Balasubramaniam, and C. V. Krishnamurthy, “Structural health monitoring of composite structures using Lamb wave tomography,” Smart materials and structures 13(5): N73. (2004)
9. J.E. Michaels, and A.J. Dawson, “Approaches to hybrid SHM and NDE of composite aerospace structures,” In SPIE Smart Structures and Materials Nondestructive Evaluation and Health Monitoring. International Society for Optics and Photonics, pp. 906427. (2014)
10. T.E. Michaels, J.E. Michaels, and M. Ruzzene, “Frequency–wavenumber domain analysis of guided wavefields”. *Ultrasonics*, *51*(4), pp.452-466. (2011)
11. O. Mesnil, C. Leckey, and M. Ruzzene, “Instantaneous and local wavenumber estimations for damage quantification in composites,” Structural Health Monitoring, 1475921714560073. (2014)
12. P. Juarez, and C. Leckey, “Multi-frequency local wavenumber analysis and ply correlation of delamination damage,” Ultrasonics 62: 56-65. (2015)
13. E. Flynn, “Embedded Multi-Tone Ultrasonic Excitation and Continuous-Scanning Laser Doppler Vibrometry for Rapid and Remote Imaging of Structural Defects." EWSHM-7th European Workshop on Structural Health Monitoring. (2014)
14. Z. Tian, C. Leckey, and L. Yu, “Phased array beamforming and imaging in composite laminates using guided waves,” In SPIE Smart Structures and Materials+ Nondestructive Evaluation and Health Monitoring. International Society for Optics and Photonics, pp. 980505. (2016)
15. O. Mesnil, and M. Ruzzene, “Sparse wavefield reconstruction and source detection using Compressed Sensing." Ultrasonics 67: 94-104. (2016)
16. Z. Tian, L. Yu, and C. Leckey, “Rapid guided wave delamination detection and quantification in composites using global-local sensing. *Smart Materials and Structures*, *25*(8), p.085042. (2016)
17. S. Chakrapani, D. Barnard, V. Dayal, “Detection of In-plane fiber waviness in composite laminates using guided lamb modes,” in Review of Progress in Quantitative Nondestructive Evaluation, New York: AIP Publishing, pp. 1134-1140. (2014)
18. L. Schmerr, “Fundamentals of Ultrasonic Nondestructive Evaluation: A modeling approach”, New York: Plenum Press. (1998)
19. F. Fellinger, and K.J. Langenberg, “Numerical techniques for elastic wave propagation and scattering,” in Elastic Waves and Ultrasonic Nondestructive Evaluation, S.K. Datta, J.D. Achenbach, and Y.S. Rajapakse, eds. Amsterdam: Elsevier, pp. 81-86. (1990)
20. R. Marklein, R. Barmann,. and K.J. Langenberg, “The Ultrasonic Modeling Code EFIT as Applied to Inhomogeneous Dissipative and Anisotropic Media,” in Review of Progress in Quantitative Nondestructive Evaluation 14B, D.O. Thompson and D.E. Chimenti, eds. New York: Plenum Press, pp. 251-258. (1995)
21. F. Schubert, A. Peiffer, and B. Kohler, “The Elastodynamic Finite Integration Technique for Waves in Cylindrical Geometries.” J Acous Soc Amer 104: 2604-2614. (1998)
22. S. Halkjaer, “Elastic Wave Propagation in Anisotropic Inhomogeneous Materials”, Ph.D. Dissertation, Technical University of Denmark, Lyngby Denmark. (2000)
23. C. Leckey, M. Rogge, and F.R. Parker. “Guided waves in anisotropic and quasi-isotropic aerospace composites: Three-dimensional simulation and experiment,” Ultrasonics, 54(1):385-394. (2014)
24. F. Quintanilla Hernando, M. J. S. Lowe, and R. V. Craster. "Modeling guided elastic waves in generally anisotropic media using a spectral collocation method." The Journal of the Acoustical Society of America 137.3, pp. 1180-1194. (2015)
25. J.P. Fuhr, J. Baumann, F. Hartel, P. Middendorf, N. Feindler, “Effects of in-plane waviness on the properties of carbon composites – experimental and numerical analysis,” 6th International Conference on Composites Testing and Model Identification pp. 61. (2013)
26. C. Leckey, P. Juarez, “Ultrasonic NDE Simulation for Composite Manufacturing Defects” in Proceedings of the American Society for Composites, 2016 *in press*